Energy management and load profile optimisation of 10 kWh BESS integrated into a Smart Polygeneration Grid subnetwork

Martina Raggio[1*], *Carlo Alberto* Niccolini Marmont Du Haut Champ[1], and *Tommaso* Reboli[1], *Paolo* Silvestri[1], *Mario Luigi* Ferrari[1]

[1] University of Genoa, TPG, Genova, Italy

Abstract. Smart Polygeneration Grids integrate different prime movers, such as traditional generators, renewable energy sources and energy storage systems to locally supply electrical and thermal power to achieve high conversion efficiencies and increase self-consumption. Integrating different energy systems poses some challenges on the plant Energy Management Systems (EMS), which must accommodate different operational requirements while following the electrical and thermal loads. Battery Energy Storage Systems (BESSs) can provide additional flexibility to the system. This paper intends to evaluate the impact of integrating a Ni-Zn-based BESS into an existing cogeneration plant through a dedicated sensitivity analysis over the operative characteristics of the BESS itself (maximum power and capacity). The IES LAB of the Savona's Campus already contains different energy systems: a cogenerative micro gas turbine, a heat-pump, solar thermal panels and two thermal energy storage systems that provide electricity and thermal power to the Smart Polygeneration Grid of the Campus. A new developed energy scheduler accommodates the integration of the new battery and meets the electrical and thermal demands. The aim is to demonstrate that integrating the BESS provides additional benefits in the system management and can reduce fuel usage and OPEX.

1 Introduction

Reducing greenhouse gas emissions and mitigating climate change has become increasingly urgent in recent years. One sector that contributes significantly to these emissions is the building one, which accounts for about 40% of global greenhouse gas emissions [1]. To address this issue, it is essential to adopt sustainable energy systems in buildings to reduce energy consumption and emissions. One solution to lower buildings emissions by 2050 is to adopt renewable energy sources and distributed energy systems [2]. These systems provide a more efficient and sustainable alternative to traditional power grids. In particular, micro gas turbines and cogeneration systems have proven effective in reducing emissions and maximising energy efficiency. Additionally, energy storage systems such as thermal and battery storage play a crucial role in balancing energy demand and supply [3].

* Corresponding author: martina.raggio@edu.unige.it

This paper focuses on developing the energy management system (EMS) for an existing plant of the Innovative Energy System Laboratory (IES LAB) of the Savona Campus. As part of the European project LOLABAT [4], a NiZn battery pack will be integrated into the plant, thus requiring a modification of the current EMS. NiZn batteries are an attractive option due to their high energy density, longer lifespan, and lower cost compared to other battery technologies [4]. The capacity of the actual NiZn battery that will be added to the system is 10kWh, but also, larger sizes are considered in the simulations (50kWh and 100kWh). Managing energy produced by different generators and using different energy storage devices can pose a significant challenge, especially in cogenerative plants. There are different possible approaches for managing a microgrid [5]. The approach used in this study considers the following steps in accordance with [6]:

1. *Day-ahead scheduling* (timescales: ~ 30 minutes/1 hour): it represents an offline optimisation to estimate the scheduling of the energy systems the day before the operation. This step is crucial in providing a high-level indication of the plant operation for the following day. Although this study focuses on the management of an existing plant, this same optimiser could also be used to assess the plant economic feasibility and optimal sizing if the capital costs and different representative days are considered over the plant lifetime.
2. *Intermediate control* (timescales: ~ 5-15 minutes): this represents the online EMS that readjusts the optimal setpoints considering updated forecasted conditions (i.e., new energy demands, prices and ambient conditions) and energy storage systems state of charge (SOC). The optimisation is performed over a future window (typically a day), and it is essential to schedule the energy storage systems operation correctly. The approach is the same as the offline scheduler, but in this case, the optimiser is updated with the new forecasted and SOCs. In this case, although the optimisation is performed over a future optimisation window, the returned outputs set points are the only referred to the immediately following time step.
3. *Real-time adjustments* (timescales: seconds): this is also an online control, but it is used to compensate for errors between real demand and the EMS signal. Typically, PID controllers can be used to this goal.

In this paper, an optimisation tool is developed for offline calculating the optimised energy scheduling (step 1). A fast optimisation tool is developed here to employ this optimiser as online EMS in future studies. This paper aims to demonstrate the benefits of adding the battery to the system, to perform a sensitivity analysis on the battery size, and provide the structure for the optimiser for the future EMS.

2 Plant layout and components characteristics

The main components of the IES LAB are:

- an AE-T100 micro gas turbine (mGT), a combined heat and power (CHP) unit which can provide in nominal conditions 100 kW_{el} and 160 kW_{th} with a nominal electrical efficiency of 30% and overall cogenerative efficiency of 80%;
- a latent heat water thermal energy storage system (TES) of 5 m^3 of capacity for the heat storage, resulting in around 150 kWh of maximum thermal capacity (with a thermal swift of around 25 K);
- a heat pump (HP), which requires 10kW_{el} and can provide 46kW_{th} (when the low heat source is at temperature of 35/40°C). The HP exploits the heat from solar façade panels as a low temperature source and is connected to another intermediate TES of the same capacity to balance the panels thermal fluctuations.

- a BESS of 10 kWh – C_{rate} = 1. This BESS is a Ni-Zn based storage which characteristics of safety, low degradation, very high DOD makes this technology suitable for a energy balance application.

The LOLABAT project consists of including a NiZn battery into this existing plant and to assess its benefits [4]. In this initial study, the complex operation of the HP integrated with the solar panel is not considered to evaluate the benefits of integrating two energy storage systems, on both thermal and electrical sides, with a micro gas turbine. The integration of the HP will be considered in future studies and the benefits of integrating the battery energy storage systems (BESS) will be also assessed. The considered layout for this initial analysis consists of the mGT, TES and BESS as shown in **Figure *1***.

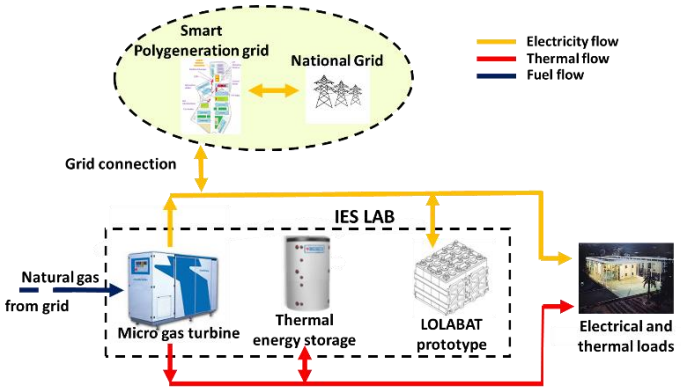

Figure 1. Plant layout

The plant is electrically connected to the "Smart Polygeneration Microgrid" (SPM) of UNIGE University Campus (Savona, Italy) which can share electricity to the national grid. The plant components electrically connected to the SPM grid are the mGT and BESS. On the thermal side, the plant is connected to a third generation DHN, where water feeds the system at around 75 °C and returns at around 50 °C.

3 Scenario

To identify a scenario to test the energy management system, the following data need to be defined:

- Electrical and thermal demands, $\boldsymbol{P}_{el-DEMAND}(\boldsymbol{T})$, $\boldsymbol{P}_{th-DEMAND}(\boldsymbol{T})$;
- Ambient temperature $\boldsymbol{T}_{amb}$, $(\boldsymbol{T})$
- Electricity costs to buy from or sell to the grid $\mathbf{C}_{\mathrm{el-GRID-buy}}(\mathbf{T})$, $\mathbf{C}_{\mathrm{el-GRID-sell}}(\mathbf{T})$
- Fuel (natural gas) cost C_{NG}

Where $\boldsymbol{T} = [t_1, t_2, \dots, t_{i-1}, t_i, t_{i+1}, \dots, t_{N-1}, t_N]$ is a vector representing the time. For this study, the considered time interval ΔT is 1 hour, therefore, N=24. The load profiles and ambient conditions are taken from typical days referred to past operations of the Savona Campus. The electrical demands have been scaled down due to the smaller size of the IES LAB compared to the SPM**.** The electricity for buying from the grid and fuel costs are taken from the Gestore Mercati Energetici (GME) website [7], the authority operating the Italian electrical energy and natural gas markets. The electricity cost is variable during the day while the natural gas cost is constant. The electricity costs for selling are obtained by multiplying the buying price with a selling-buying ratio. A representative day of April 2022 was selected, where the variable electricity prices are shown in Figure 2.

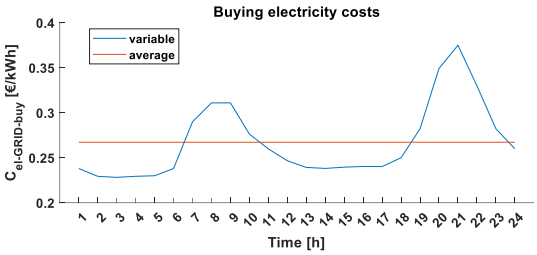

Figure 2. Variable electricity costs of a representative day of April and the averaged value [7].

4 Components performance functions and costs

The optimiser requires components specifications and operational costs to calculate the overall daily plant costs. A dynamic Simulink model of each component of the plant was previously developed and validated as part of the ENVISION project [8,9]. The performance functions have been simplified to reduce the computational time of the optimiser.

4.1 Micro gas turbine

The micro gas turbine performance is calculated with the same off-design curves of the previously Simulink validated model. There is a one-to-one correspondence between electrical power $\boldsymbol{P}_{el-mGT}$ and thermal power $\boldsymbol{P}_{th-mGT}$ produced by the mGT. For this specific problem formulation (described in Paragraph 5), it is required to use a performance function, f_{MGT}, that calculates the $\boldsymbol{P}_{el-mGT}$ as a function of $\boldsymbol{P}_{th-mGT}$. If the $\boldsymbol{P}_{th-mGT}$ produced is more than the demand and the TES cannot store the excess of energy, a bypass-valve at the exhausts opens to release the unused energy. When $\boldsymbol{x}_{bypass-mGT}$=0 the bypass valve is fully open and 1 the valve is fully closed. The fuel mass flow is also required to calculate the costs due to the mGT operation. Therefore, the mGT performance function has this general structure:

$$[\boldsymbol{P}_{el-mGT}, \boldsymbol{m}_{fuel-MGT}] = f_{MGT}(\boldsymbol{T}_{amb}, LHV_{fuel}, \boldsymbol{P}_{th-mGT}) \quad (1)$$

The minimum electrical power output of the mGT corresponds to the minimum environmental load, below which unacceptable emissions of CO are produced, while the maximum power output depends on the ambient temperature, and it is around the nominal value of 100 kW. The costs related to the mGT operations are not only linked to the fuel mass flow rate utilised but also to the variable operational costs $OPEX_{Var-mGT} = 0.015\ €/kWh$, whose value is in accordance with ref. [10].

4.2 Thermal energy storage

The TES system is used to store and release thermal energy based on the requested thermal power $\boldsymbol{P}_{th-TES-req}$ (according to the considered convention, positive during the discharge and negative during the charge). The TES performance function has this general structure:

$$[\boldsymbol{E}_{th-TES}, \boldsymbol{P}_{th-TES}] = f_{TES}(SOC_{TES-t0}, SOC_{TES-tN}, \mathrm{E}_{\mathrm{th-TES-min}}, \mathrm{E}_{\mathrm{th-TES-max}}, \boldsymbol{P}_{th-TES-req}, \Delta T) \quad (2)$$

The function calculates the thermal capacity $\boldsymbol{E}_{th-TES-out}$ and power output $\boldsymbol{P}_{th-TES}$ of the TES based on the initial and final state of charge SOC_{TES-t0} and SOC_{TES-tN}, the minimum and maximum thermal capacity $\mathrm{E}_{\mathrm{th-TES-min}}$ and $\mathrm{E}_{\mathrm{th-TES-max}}$, the requested power

$\boldsymbol{P}_{th-TES-req}$ and the time interval ΔT. A circularity is imposed so that $SOC_{TES-t0} = SOC_{TES-tN}$.The formula used to calculate each component of $\boldsymbol{E}_{th-TES}$ is:

$$E_{th-TES}(t_i) = E_{th-TES}(t_{i-1}) - P_{th-TES-req}(t_i) * \Delta T \quad (3)$$

If the requested power exceeds the capability of the storage (if $E_{th-TES-out}(t_i) < \mathrm{E_{th-TES-min}}$ or $E_{th-TES-out}(t_i) > \mathrm{E_{th-TES-max}}$), the thermal capacity only reaches its minimum or maximum value ($E_{th-TES-out}(t_i) = \mathrm{E_{th-TES-min}}$ or $E_{th-TES-out}(t_i) = \mathrm{E_{th-TES-max}}$). The real power output $\boldsymbol{P}_{th-TES}$ is calculated by rearranging equation (**3**) with the updated $E_{th-TES-out}(t_i)$ values.
The variable OPEX for the TES are negligible due to non-moving parts [11] while the fixed maintenance cost is not considered for the optimisation, being that a constant value.

4.3 Battery storage

The battery performance is modelled with the same approach of the TES. In this case the structure is the following:

$$[E_{el-BEES}, P_{el-BEES}] = f_{TES}(SOC_{BESS-t0}, SOC_{BEES-tN}, \eta_{BESS}, SOC_{BEES-tN}, E_{el-BEES-min}, E_{el-BEES-max}, P_{el-BEES-req}, \Delta T) \quad (4)$$

The battery efficiency η_{BESS} considered here and assumed to be equal for both charging and discharging. The formula used to calculate each component of the $\boldsymbol{E}_{el-BEES-out}$ vector is:

$$E_{th-TES}(t_i) = E_{th-TES}(t_{i-1}) - \eta_{BESS} * P_{th-TES-req}(t_i) * \Delta T \quad (5)$$

If the requested power exceeds the capability of the storage the battery only reaches its minimum or maximum value. The real power output is calculated rearranging equation (**5**). For simplicity, the OPEX are not considered in this study.

5 Parameters constraints, cost function and optimiser

The main problem constraints are the energy balances:

$$\boldsymbol{P}_{el-DEMAND} - \boldsymbol{P}_{el-GRID} - \boldsymbol{P}_{el-mGT} - \boldsymbol{P}_{el-BESS} = \boldsymbol{0} \quad (6)$$
$$\boldsymbol{P}_{th-DEMAND} - \boldsymbol{x}_{bypass-mGT} * \boldsymbol{P}_{th-mGT} - \boldsymbol{P}_{th-TES} = \boldsymbol{0} \quad (7)$$

The only decision variables for this problem are $\boldsymbol{P}_{el-TES-req}$, $\boldsymbol{P}_{el-BESS-req}$ and $\boldsymbol{x}_{bypass-mGT}$ while $\boldsymbol{P}_{el-GRID}$ and $\boldsymbol{P}_{th-mGT}$ can be calculated from the two energy balances. In combination with the energy balance constraints, the upper and lower boundaries should also be respected as indicated in Table 1. It was also imposed only one startup for the mGT per day since repetitive shutdowns and startup can negatively affect the life duration and maintenance costs.

Table 1. Parameters lower and upper boundaries

Parameter	Unit	Min value	Max value
Electricity exchanged with the grid, $\boldsymbol{P_{el-GRID}}$	[kW]	-200	+200
Micro gas turbine electrical power output, $\boldsymbol{P_{el-mGT}}$	[kW]	+20	$f(T_{amb})$
Micro gas turbine bypass valve closing	[-]	0	+ 1
Thermal energy storage exchanged power, $\boldsymbol{P_{th-TES}}$	[kW]	-150	+150
Battery exchanged power, $\boldsymbol{P_{el-BESS}}$	[kW]	-10	+10

The total cost for operating the plant is calculated as below:

$$\mathrm{COST_{TOT}} = \Delta T \sum_{i=1}^{N} \left(C_{el} * P_{el-GRID}(t_i) + m_{fuel-mGT}(t_i) * C_{NG} * LHV_{NG} + OPEX_{Var-mGT} * P_{el-mGT}(t_i) \right) \quad (8)$$

Where $C_{el} = \begin{cases} C_{el-GRID-buy}(t_i) & if\ (P_{el-GRID}(t_i) \geq 0) \\ C_{el-GRID-sell}(t_i) & if (P_{el-GRID}(t_i) < 0) \end{cases}$

The optimiser used in this study to calculate the optimal values of $\boldsymbol{P}_{el-TES-req}$, $\boldsymbol{P}_{el-BESS-req}$ and $\boldsymbol{x}_{bypass-mGT}$ is the particle-swarm algorithm, a widely used metaheuristic optimisation algorithm used for different energy scheduling problems [12]. The algorithm generates a random initial guess and iteratively modifies $\boldsymbol{P}_{el-TES-req}$, $\boldsymbol{P}_{el-BESS-req}$ and $\boldsymbol{x}_{bypass-mGT}$ to reach the minimum value of the cost function $\mathrm{COST_{TOT}}$. At each iteration, to calculate the cost function, $\boldsymbol{P}_{el-TES}$ and $\boldsymbol{P}_{el-BEES}$, are calculated with equations (**2**) and (**4**). Then, from the thermal energy balance of equation (**7**) is calculated $\boldsymbol{P}_{th-mGT}$ and equation (**1**) yields $\boldsymbol{m}_{fuel-mGT}$ and $\boldsymbol{P}_{el-mGT}$. Finally, the electrical energy balance equation (**6**) determines $\boldsymbol{P}_{el-GRID}$. The obtained values of $\boldsymbol{P}_{el-GRID}$, $\boldsymbol{P}_{el-mGT}$ and $\boldsymbol{m}_{fuel-mGT}$ are used to calculate the total cost (equation (**8**)). The optimiser will return the optimal values $\boldsymbol{P}_{el-TES-req}$ and $\boldsymbol{P}_{el-BESS-req}$, $\boldsymbol{x}_{bypass-mGT}$ from which the optimal final values $\boldsymbol{P}_{el-GRID}$ and $\boldsymbol{P}_{el-mGT}$ can be calculated with a similar approach.

6 Results

Table 2 presents a comparison of different scenarios for a microgrid system that includes the micro gas turbine (AE-T100), TES, and BESS; moreover, a sensitivity analysis with different energy storage capacities (10kWh, 50kWh, and 100kWh) is performed. The table compares the baseline scenario (T100 and TES only) with the scenarios that include BESS with different energy storage capacities. The size of the battery was increased by keeping the same maximum C_{rate}=1. The parameter $ratio_{\textbf{sell-buy}}$ stands for the ratio between selling and buying grid electricity costs and it depends on the specific contract of the microgrid. Two extreme cases where considered: a value of 0, meaning that the system can still provide excess electricity to the grid without revenue, and a value of 1, meaning that the cost of selling electricity to the grid equals the cost of buying electricity from the grid. A positive value of the absolute and relative savings indicates cost savings. The table demonstrates that adding a battery to the microgrid can lead to significant cost savings, mainly when the ratio between selling and buying grid electricity costs is low. Additionally, as the energy storage capacity increases, the cost savings increase in both absolute and relative terms.

Table 2. Plant costs and savings with sensitivity analysis the BESS size

Parameter	**Unit**	**T100 and TES (baseline)**		**T100, TES and BESS (10kWh)**		**T100, TES and BESS (50kWh)**		**T100, TES and BESS (100kWh)**	
$Ratio_{sell-buy}$	[-]	0	1	0	1	0	1	0	1
Plant total cost	[€]	510.9	480.1	501.8	470.8	489.7	463.1	486.8	453.5
mGT total cost	[€]	325.4	385.8	328.2	384.7	334.0	383.9	331.4	384.3
Grid total cost	[€]	185.5	94.2	173.5	86.1	155.6	79.2	155.4	69.1
Saving from baseline (abs.)	[€]	0	0	+9.1	+9.2	+21.2	+16.9	+24.1	+26.5
Saving from baseline (rel.)	[%]	0	0	+1.78	+1.92	+4.15	+3.53	+4.71	+5.53

Figure 3 recaps the main outcomes of the analysis, in terms of relative savings. In accordance with Table 2, is possible to highlight that the integration of a Ni-Zn-based BESS is ever beneficiary for the plant, allowing to reach a saving up to 5.5% of the baseline cost. It must be highlighted that for the intermediate capacity (50 kWh) the saving is higher with

a value of $ratio_{sell\text{-}buy}$ = 1, contrary to what happens with 100 kWh capacity. The difference between the two different values of $ratio_{sell\text{-}buy}$ with a BESS of 10 kWh seems to be negligible.

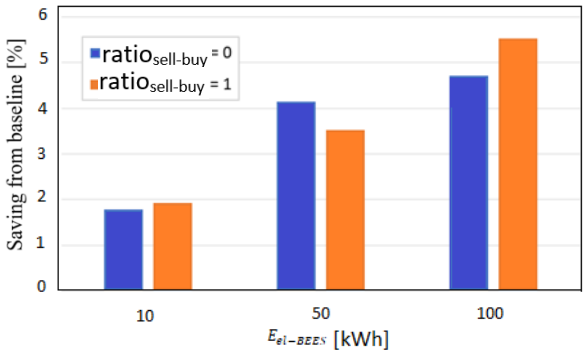

Figure 3. Savings from baseline as function of the BESS capacity.

Figure 4 and Figure 5 display the electrical and thermal power scheduling with a 50 kWh BESS (intermediate case) with a $ratio_{sell\text{-}buy}$ equal to 0 and 1, respectively. Both scenarios start with SOC_{TES} and SOC_{BESS} equal to 0. Saving from baseline [%]

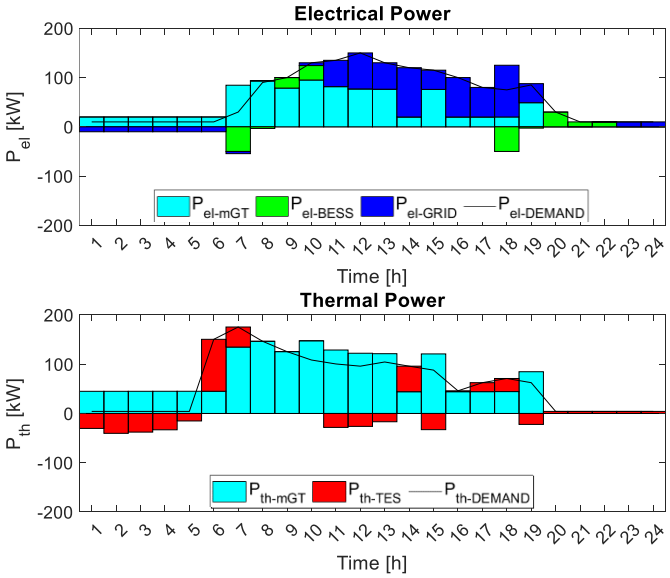

Figure 4. Electrical and thermal power scheduling when with a 50 kWh BESS and $ratio_{sell\text{-}buy}$=0

In Figure 4, the mGT turns on from t = 1 to 5 hours to satisfy the low electrical and thermal demand. The mGT operates at minimum load, injecting the unused electricity to the grid without revenue and charging the TES with the excess of produced thermal power. At t= 6 hours, the mGT still operates at minimum load due to the low electrical demand and the increased thermal demand is satisfied by both mGT and TES. At t=7, the mGT increases the load since the TES is almost discharged and cannot satisfy the thermal demand alone. The battery charges with the unused electricity and discharges at t=9 and t=10 hours when the price is higher, thus reducing the purchased power. During the central hours, the electricity price is low, and the mGT runs at a high load only to satisfy the thermal power and charge the TES for later use. At t=18 hours, the electricity price is still low and electricity is bought

to charge the battery, which is discharged later when the price increases. During the last hours of the day, from t=20 to 24 hours, electrical demand is satisfied by the battery and grid and the thermal demand only with the TES.

In Figure 5, the BESS charging and discharging schedule is changed. At t= 5, when the electricity price is still low the battery charges and discharges at t= 8 hours when the electricity price is low. Again at t=17 hours, electricity is bought at low price to charge the battery and it is discharged at t=21 hours , where the electricity is the highest. A t= 8,9 and 20,21 hours, corresponding to the electricity price peaks, also, the mGT is run a full load to exploit the overall plant revenue even when the thermal demand is lower than what is provided by the mGT.

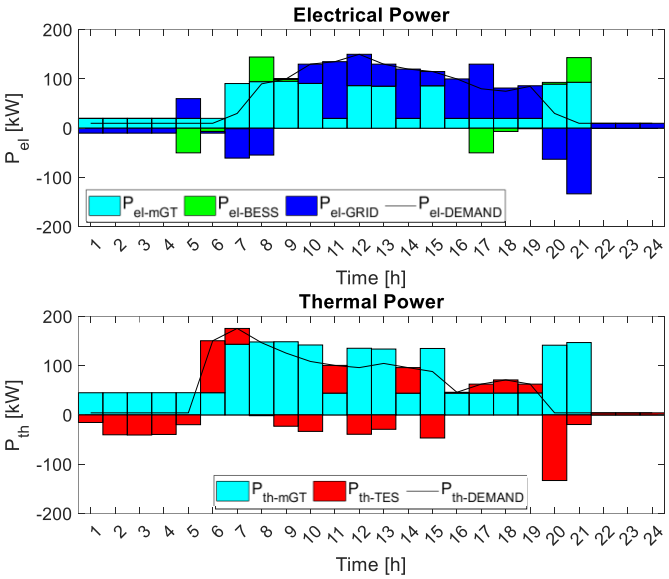

Figure 5. Electrical and thermal power energy when with a 50 kWh BESS and $ratio_{sell\text{-}buy}$=1

7 Conclusions

In the present work, a novel EMS is devised to optimize the energy fluxes between a cogenerative plant and the electrical market to maximize its profitability. In detail, the initial original plant features a mGT together with a TES which then are integrated with a Ni-Zn based BESS. By relying on such energy scheduler, several simulations are performed in different scenarios which involve variable electrical market parameters like electricity purchasing cost and selling price in terms of sell buy ratio; in this way, the best plant strategy which maximizes plant economical revenue can be found and then implemented in real-time by relying on a suitable plant control system. The obtained results show that by adding the Ni-Zn based BESS to the original energy system, an economical saving is obtained with respect to plant baseline cost which increases in a monotonic way with BESS capacity. Moreover, such economical saving depends even on the current electricity market sell buy ratio but, in this case, further developments are needed to better assess the influence of this parameter.

The next steps of this work can be adding a sensitivity analysis over the C_{rate}, Depth of Discharge (DoD) and number of the BESS and over the $ratio_{sell\text{-}buy}$ parameter. In fact, extending the analysis over these two parameters will help to better quantify and maximize the performance of the plant.

8 Acknowledgements

This project has received funding from the European Union's Horizon Europe research and innovation programme under grant agreement No 963576, LOLABAT. Views and opinions expressed are however those of the author(s) only and do not necessarily reflect those of the European Union or of CINEA.

References

[1] M. Rivarolo, D. Rattazzi, L. Magistri, A.F. Massardo, Multi-criteria comparison of power generation and fuel storage solutions for maritime application, Energy Convers. Manag. 244 (2021) 114506
[2] D. D'Agostino, P. Zangheri, L. Castellazzi, Towards nearly zero energy buildings in Europe: A focus on retrofit in non-residential buildings, Energies. 10 (2017).
[3] D. Bellotti, M. Rivarolo, L. Magistri, A comparative techno-economic and sensitivity analysis of Power-to-X processes from different energy sources, Energy Convers. Manag. 260 (2022) 115565.
[4] LOLABAT - Bringing NiZn back, (n.d.). https://www.lolabat.eu/.
[5] A. Bouakkaz, A.J.G. Mena, S. Haddad, M.L. Ferrari, Efficient energy scheduling considering cost reduction and energy saving in hybrid energy system with energy storage, J. Energy Storage. 33 (2021) 101887.
[6] T. Reboli, M. Ferrando, L. Mantelli, L. Gini, A. Sorce, J. Garcia, R. Guedez, GAS TURBINE COMBINED CYCLE RANGE ENHANCER - PART 1: CYBER-PHYSICAL SETUP, (2022) 1–15.
[7] GME, GME - Gestore dei Mercati Energetici, (2016) 9–10. https://www.mercatoelettrico.org/it/%0Ahttp://www.mercatoelettrico.org/En/Default.aspx.
[8] C. Anfosso, L. Gini, D. Bellotti, M. Pascenti, L. Magistri, Energy Proceedings Experimental results of an innovative NIR-solar façade panels-based polygeneration system, 28 (2022).
[9] C. Anfosso, L. Gini, D. Bellotti, L. Magistri, Dynamic model validation of an innovative NIR-solar facade panels-based integrated system, Energy Procedia 2022.
[10] M. Montero Carrero, W. De Paepe, S. Bram, F. Musin, A. Parente, F. Contino, Humidified micro gas turbines for domestic users: An economic and primary energy savings analysis, energy. 117 (2016) 429–438.
[11] A. Ashfaq, A. Ianakiev, Cost-minimised design of a highly renewable heating network for fossil-free future, energy. 152 (2018) 613–626.
[12] M.Y. Ali, F. Khan, V.K. Sood, Swarm Optimization and Wireless Communication System, 2018 IEEE Electr. Power Energy Conf. (2018) 1–7.